# Modelling and Simulation of RF Multilayer Inductors in LTCC Technology

Amer Čelić

***Abstract* – This paper is aimed at presenting the models and characteristics of two types of inductors designed in LTCC (Low Temperature Cofired Ceramic) technology. We present the physical model of a 3D planar solenoid-type inductor and of a serial planar solenoid-type inductor for the RF (radio frequency) range. To verify the results obtained by using these models, we have compared them with the results obtained by employing the Ansoft HFSS electromagnetic simulator. Very good agreement has been recorded for the effective inductance value, whereas the effective Q factor value has shown a somewhat larger deviation than the inductance.**

***Keywords* - Q factor, Physical model of inductor, Inductance, Planar solenoid inductor.**

## I. Introduction

An integrated inductor is a component finding ever wider applications in low-noise amplifiers, active mixers, voltage-controlled oscillators, power converters, miniature sensors, filters, etc. [1]. The main features of an inductor are its inductance and Q factor.

Various techniques are used for fabricating a component or circuit, depending on their characteristics and dimensions to be achieved as well as on the place of their intended use. Technologies used most commonly for producing microstructures are monolithic technology [2], thick-film technology [3] and *low temperature cofired ceramic* (LTCC) technology [4], [5]. A designer of microelectronic structures should be familiar with as many technologies as possible to be capable of selecting a technology that will give the optimal characteristics of a designed component. In addition to various technologies, a designer's knowledge should also include the electrical characteristics describing an inductor.

The aim of this paper is to derive a physical model of two types of planar solenoid inductors for operation in the radio frequency range. The simulation of inductor structures using electromagnetic simulators can give data on the effective values of inductance and Q factor as well as on resonance frequency, but it cannot provide information on parameters such as series resistance, series capacitance, parasitic capacitance to the substrate, etc. This is why deriving the physical model of an inductor can show exactly how these values affect the effective values of its inductance and Q factor. The verification of results obtained on the basis of physical model has been performed by using the *Ansoft HFSS* electromagnetic simulator [6].

A. Čelić, Faculty of Technical Sciences in Novi Sad, Serbia (e-mail: celicamer@yahoo.com).

## II. Deriving the Physical Model of an Inductor Designed for LTCC Technology

The view of inductor structures designed for LTCC technology is shown in Figure 1.

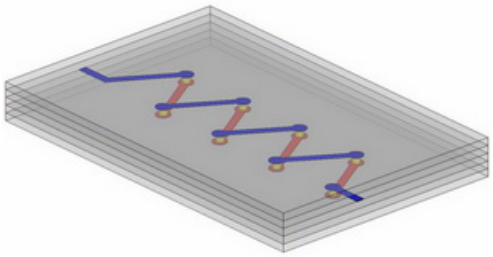

(a) 3D Inductor.

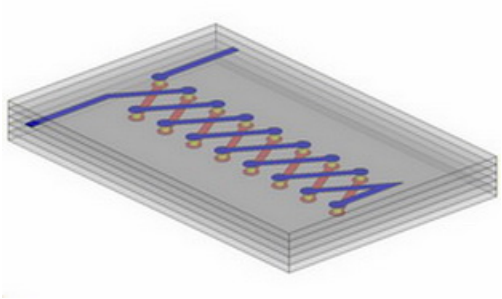

(b) Serial Inductor.

Fig. 1. 3D View of Inductor Structures.

As may be seen from Figure 1, inductor structures have been designed using five dielectric stripe produced by DuPont company – DuPont 951PT [7]. DuPont's silver pastes DuPont 6142D [7] were used for conducting lines. Inductors were designed so as to have the same conducting line widths (100μm), the same conducting line thicknesses (9μm) and to occupy identical areas on a chip. Via diameter was 100μm. Both inductors had the same dimensions (5.4 x 2.2 x 0.5)mm.

Knowledge of the physical model of inductor is very important for its application, because it permits recognizing all the characteristic parameters affecting the inductor. Precise inductor modeling is rather demanding because of numerous parasitic effects occurring at high frequencies [8].

Figure 2 presents the physical structure of 3D inductor with the characteristic parameters describing the inductor at high frequencies (series inductance $L_S$, series resistance $R_S$, series capacitance $C_S$, parasitic capacitance to the substrate $C_K$), and Figure 3 its equivalent π-diagram. The physical structure and equivalent π-diagram of serial inductor are identical to those of 3D inductor.

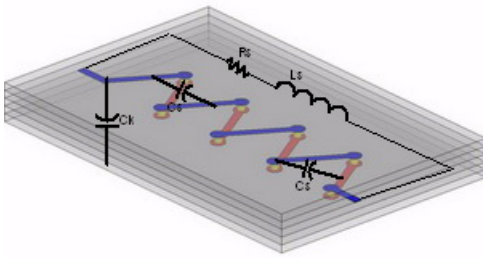


Fig. 2. Physical Structure of 3D inductor.

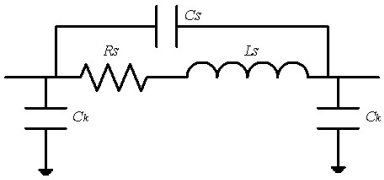


Fig. 3. Equivalent π-diagram of 3D inductor.

Series inductance $L_S$ is the sum of the selfinductances of inductor's single segments ($L_O$) and the mutual inductances between the parallel and acute line segments of inductor ($L_{M1} + L_{M2}$),

$$L_S = L_{OU} + L_{M1U} + L_{M2U}. \tag{1}$$

The selfinductance of one line segment is obtained using equation (2) and the total selfinductance ($L_{OU}$) by summing the selfinductances of all single line segments with the selfinductance introduced by vias ($L_{via}$), equation (3),

$$L_O = \frac{\mu_O l_l}{2\pi}\left[\ln\frac{2l_l}{w_l + t_l} + 0{,}50049 + \frac{w_l + t_l}{3l_l}\right], \tag{2}$$

$$L_{via} = \frac{\mu_o \mu_r}{2\pi}\left[t_{via}\sinh^{-1}\left(\frac{t_{via}}{w_{via}}\right) - \sqrt{t_{via}^2 + w_{via}^2} + w_{via}\right], \tag{3}$$

where $l_l$, $w_l$, $t_l$ are the lengths, widths and thicknesses of line segments, respectively, $w_{via}$ and $t_{via}$ are via diameter and length, and $\mu_r = 0.99998$ is the relative permeability of conducting line.

Mutual inductance between two parallel inductor segments is obtained by using equation (4) and the total mutual inductance ($L_{M1U}$) by summing the single mutual inductance between parallel segments (9),

$$L_{M1} = \frac{\mu_O \mu_r}{2\pi} l_l\left[\ln\left(\frac{l_l}{G} + \sqrt{1 + \frac{l_l^2}{G^2}}\right) - \sqrt{1 + \frac{G^2}{l_l^2}} + \frac{G}{l_l}\right], \tag{4}$$

where parameter $G$ is given by equation (5),

$$\ln G = \ln d - \left[\left(\frac{1}{12(d/w_l)^2}\right) + \left(\frac{1}{60(d/w_l)^4}\right) + \left(\frac{1}{164(d/w_l)^6}\right)\right], \tag{5}$$

and $d$ is the distance between parallel segments.

Mutual inductance between the two segments of an inductor that are positioned at an angle $\varphi$, Figure 4, is obtained by using equation (6) and the total mutual inductance ($L_{M2U}$) by summing the single mutual inductance between these segments [9],

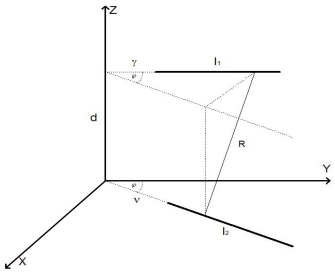


Fig. 4. Slant Segments at an Angle $\varphi$.

$$L_{M2} = \frac{\mu_o \cos\varphi}{4\pi}[2[(\gamma + l_1)arth\left(\frac{l_2}{R_1 + R_2}\right) + (\upsilon + l_2)arth\left(\frac{l_1}{R_1 + R_4}\right) - \mu arth\left(\frac{l_2}{R_3 + R_4}\right) - \upsilon arth\left(\frac{l_1}{R_2 + R_3}\right)\Big] - \frac{\Omega d}{\sin\varphi}\Big], \tag{6}$$

where parameter $\Omega$ is given by equation (7)

$$\Omega = arctg\left(\frac{d^2\cos\varphi + (\gamma + l_1)(\upsilon + l_2)\sin^2\varphi}{dR_1\sin\varphi}\right) - arctg\left(\frac{d^2\cos\varphi + (\gamma + l_1)\upsilon\sin^2\varphi}{dR_2\sin\varphi}\right) + arctg\left(\frac{d^2\cos\varphi + \gamma\upsilon\sin^2\varphi}{dR_3\sin\varphi}\right) - arctg\left(\frac{d^2\cos\varphi + \gamma(\upsilon + l_2)\sin^2\varphi}{dR_4\sin\varphi}\right), \tag{7}$$

and auxiliary parameters $R_1$, $R_2$, $R_3$, $R_4$ are given by equation (8),

$$\begin{aligned} R_1^2 &= d^2 + (\gamma + l_1)^2 + (\upsilon + l_2)^2 - 2(\gamma + l_1)(\upsilon + l_2)\cos\varphi, \\ R_2^2 &= d^2 + (\gamma + l_1)^2 + \upsilon^2 - 2(\gamma + l_1)\upsilon\cos\varphi, \\ R_3^2 &= d^2 + \gamma^2 + \upsilon^2 - 2\gamma\upsilon\cos\varphi, \\ R_4^2 &= d^2 + \gamma^2 + (\upsilon + l_2)^2 - 2\gamma(\upsilon + l_2)\cos\varphi. \end{aligned} \tag{8}$$

The series resistance of 3D inductor is given by equation (9)

$$R_S = \frac{N\rho_l l_l}{2\delta(w_l + t_l)} + \frac{2\rho_l l_K}{2\delta(w_l + t_l)} + \frac{N\rho_l t_{via}}{\delta 2\pi w_{via}/2} + \frac{2N\rho_l t_l}{\pi(w_{pad})^2}, \tag{9}$$

where $N=8$ is the total number of 3D inductor's acute angles, $\rho_l$ = 2.97*10$^{-8}$ Ωm is the specific resistance of conducting line, $l_K$ is the length of connection segments and $w_{pad}$ is the diameter of extracting at terminal of conductive segment (pad). The parameter describing the dependence of resistance on frequency is referred to as skin depth $\delta$ and is given by equation (10).

$$\delta = \sqrt{\frac{\rho_l}{\pi\mu_o\mu_r f}}. \tag{10}$$

The series capacitance of 3D inductor is given by equation (11) and includes the capacitance between parallel segments, acute segments and the capacitance between extracting at terminal of conductive segment (*via pad*)

$$C_S = \varepsilon_0\varepsilon_{rk}\frac{(N-2)(l_l - t_{kor}\sin(\varphi/2))t_l}{t_{kor}\cos(\varphi/2) - w_l} + \varepsilon_0\varepsilon_{rk}\frac{(N-1)l_l t_l}{\sqrt{t_{via}^2 + (p/2)^2}} + \varepsilon_0\varepsilon_{rk}\frac{N\pi\left[(w_{pad}/2)^2 - (w_{via}/2)^2\right]}{T_{\ker}}, \tag{11}$$

where $\varepsilon_{rk}$ = 7.8 is the relative permittivity of ceramic substrate, and $T_{ker}$ = 100μm is the ceramic substrate thickness. Parasitic capacitance to the substarte is

calculated using equation (12) and exists between the inductor itself and the metal coating deposited from the lower side of the component.

$$C_K = \frac{1}{2}\varepsilon_o\varepsilon_{rk}\frac{\frac{N}{2}w_l l}{2T_{\text{ker}}} + \frac{1}{2}\varepsilon_o\varepsilon_{rk}\frac{\frac{N}{2}w_l l}{3T_{\text{ker}}} + \frac{1}{2}\varepsilon_o\varepsilon_{rk}\frac{2w_l l_K}{3T_{\text{ker}}} + \frac{1}{2}\varepsilon_o\varepsilon_{rk}\frac{N\pi\left(w_{pad}/2\right)^2}{2T_{\text{ker}}}. \quad (12)$$

These equations correspond to the physical model of 3D inductor. To calculate the values of the elements of equivalent π-diagram of serial inductor, we use the following equations. The series resistance of serial inductor is calculated on the basis of equation (13),

$$R_S = \left(N_g + N_d\right)\frac{\rho_l l_l}{2\delta\left(w_l + t_l\right)} + \frac{\rho_l l_K}{2\delta\left(w_l + t_l\right)} + \frac{2\rho_l l_p}{2\delta\left(w_l + t_l\right)} + \frac{\left(N_g + N_d\right)\rho_l t_{via}}{2\pi\delta\left(w_{via}/2\right)} + \frac{\rho_l t_l 2\left(N_g + N_d\right)}{\pi\left(w_{pad}/2\right)^2}, \quad (13)$$

where $N_g = 8$ is the total number of acute segments on the upper conducting layer, $N_d = 8$ is the total number of acute segments on the lower conducting layer, $l_p$ is the end segment connecting the segments of the upper and lower conducting layer.

The series capacitance of serial inductor is obtained on the basis of equation (14) and includes the capacitance between the parallel segments, acute segments, the capacitance between extracting at terminal of conducting segments (*via pad)* and the capacitance between the overlapping parts of the segments of the upper and lower conducting layers.,

$$C_S = \varepsilon_o\varepsilon_{rk}\frac{\left(\left(N_g + N_d\right) - 2\right)\left(l_l - t_{kor}\sin(\varphi/2)\right)t_l}{t_{kor}\cos(\varphi/2)} + \varepsilon_o\varepsilon_{rk}\frac{\left(\left(N_g + N_d\right) - 2\right)t_l t_l}{\sqrt{t_{via}^2 + t_{kor}^2}} + \varepsilon_o\varepsilon_{rk}\frac{N_g w_l^2}{T_{\text{ker}}} + \varepsilon_o\varepsilon_{rk}\frac{\left(N_g + N_d\right)\pi\left(\left(w_{pad}/2\right)^2 - \left(w_{via}/2\right)^2\right)}{T_{\text{ker}}}, \quad (14)$$

where $t_{kor}$ is the distance between the two parallel segments of serial inductor.

The parasitic capacitance to the substrate of serial inductor is calculated on the basis of equation (15)

$$C_K = \frac{1}{2}\varepsilon_o\varepsilon_{rk}\frac{N_d w_l l}{2T_{\text{ker}}} + \frac{1}{2}\varepsilon_o\varepsilon_{rk}\frac{N_g w_l l}{3T_{\text{ker}}} + \frac{1}{2}\varepsilon_o\varepsilon_{rk}\frac{2w_l l_K}{3T_{\text{ker}}} + \frac{1}{2}\varepsilon_o\varepsilon_{rk}\frac{w_l l_p}{3T_{\text{ker}}} + \frac{1}{2}\varepsilon_o\varepsilon_{rk}\frac{\left(N_g + N_d\right)\pi\left(w_{pad}/2\right)^2}{2T_{\text{ker}}}. \quad (15)$$

The effective values of the inductances and *Q factor* of 3D and serial inductors are calculated on the basis of equations (16) and (17),

$$L = \frac{\left(L_S - R_S^2\left(1 + \frac{w^2 L_S^2}{R_S^2}\right)\left(C_S + C_K\right)\right)\left(1 + \frac{w^2 L_S^2}{R_S^2}\right)}{\left(\frac{w}{R_S}\right)^2\left[L_S - R_S^2\left(1 + \frac{w^2 L_S^2}{R_S^2}\right)\left(C_S + C_K\right)\right]^2}, \quad (16)$$

$$Q = \frac{wL_S}{R_S}\left[1 - \frac{R_S^2\left(C_S + C_K\right)}{L_S} - w^2 L_S\left(C_S + C_K\right)\right]. \quad (17)$$

## III. Comparison of Results Calculated Using Inductor Model with Simulation Results

Figures 5 and 6 present a comparison of the results of the effective values of the inductance and Q factor of 3D inductor obtained by calculation of the parameters of inductor's physical model and by simulation. The same meshing was used for both inductor types in simulation.

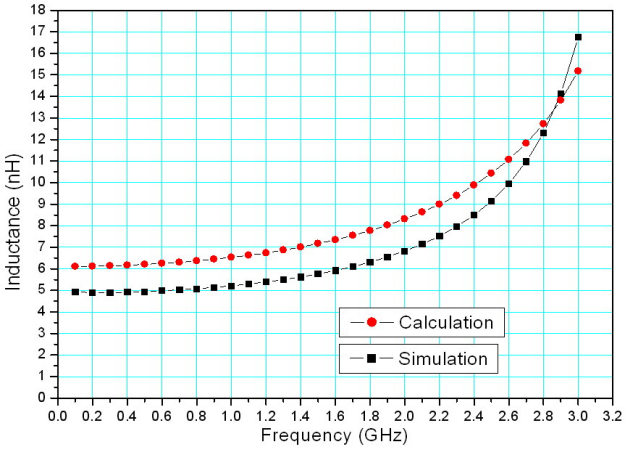


Fig. 5. Inductance of 3D Inductor.

As can be seen, in the case of 3D inductor the value of inductance obtained by calculation is slightly larger than the simulated value. The calculated inductance value of 3D inductor at 1 GHz frequency is 6.53nH. The simulated inductance value of 3D inductor at 1GHz frequency is 5.21nH. The inductance increases with the increasing frequency.

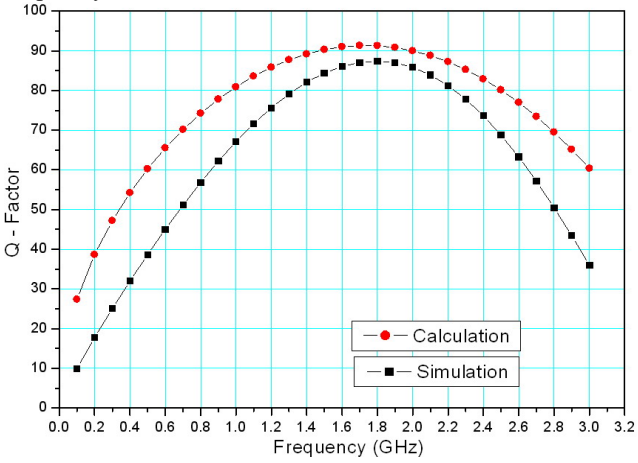


Fig. 6. Q Factor of 3D Inductor.

The maximum calculated Q factor value of 3D inductor was 91.33 and was obtained at 1.7GHz frequency. The maximum Q factor value obtained by simulation was 87.42 and was obtained at 1.8GHz. It can be seen that the deviation is very small. This is due to the fact that many parasitic effects are taken into account in the calculation.

Figures 7 and 8 present a comparison of the results of the effective values of the inductance and Q factor of serial inductor obtained by the calculation of the parameters of inductor's physical model and by simulation.

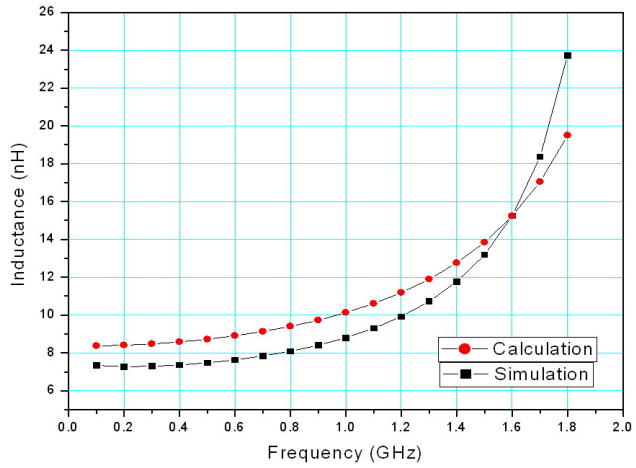


Fig. 7. Inductance of Serial Inductor.

A good agreement between the calculated and simulated inductance value was also obtained in the case of serial inductor. A slightly larger calculated inductance value was obtained compared with the simulated one. The calculated inductance value at 1GHz frequency is 10.13nH. The simulated inductance value at 1GHz frequency is 8.8nH.

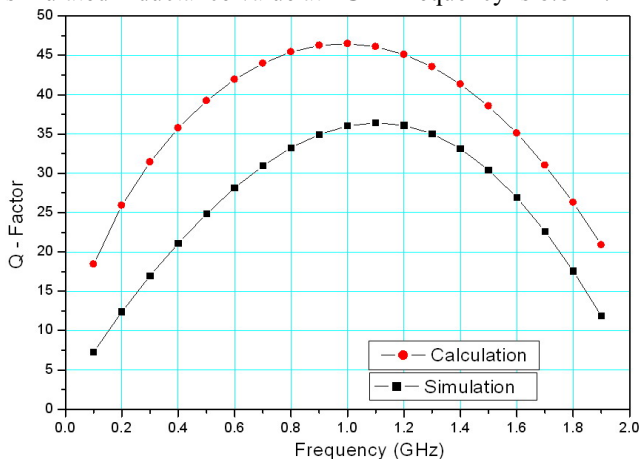


Fig. 8. Q Factor of 3D Inductor.

The maximum Q factor value obtained by calculating the parameters of the equivalent π-diagram of serial inductor was 46.47 and was obtained at 1GHz frequency. The maximum Q factor value obtained by simulation was 36.43 and was obtained at 1.1 GHz frequency. It can be noted that the deviation of the simulated Q factor value from the calculated one for the serial inductor is larger in comparison with the 3D inductor. This is so because there are a larger number of segments, and the parasitic capacitances and series resistance are therefore larger as well.

## IV. Conclusion

This paper presents the physical models and characteristics of two inductor types. The values of the calculation and simulation for the effective inductance and Q factor value are compared.

The inductance of serial inductor is larger than that of 3D inductor. This difference is introduced by the larger number of segments of serial inductor, the larger number of vias as well as the larger number of pads. The Q factor of serial inductor is lower than the Q factor of 3D inductor. This results from the higher values of the elements of the equivalent π-diagram obtained with the serial inductor compared with the 3D inductor.

Briefly, if the inductance value is a decisive criterion for the intended application of the inductor, it should be realized as a serial one; on the other hand, if the Q factor value is decisive, the inductor should be realized as a 3D inductor [9].

## ACKNOWLEDGEMENT

This paper forms part of a Master Degree Thesis and has been prepared under the supervision of Ms Ljiljana Živanov, PhD and Mr Goran Radosavljević, MS, both with the Faculty of Technical Sciences in Novi Sad. Research and results reported in the paper have been partially supported by Serbia's Ministry of Sceince and Technology Development under Grant No 11023.

## References

[1] Ch. M. Tai, Ch. N. Liao, "A Physical Model of Solenoid Inductors on Silicon Substrates," *IEEE Transactions on Microwave Ttheory and Techniques,* vol. 55, no. 12, Decebmer 2007.

[2] A. M. Niknejad, R. G. Mayer, "Analysis, design, and optimization of spiral inductors and transformers for Si RF IC's ," *IEEE Journal of Solid-State Circuits,* vol.3, no. 10 , pp. 1470-1481, October 1998.

[3] V. Desnica, Lj. Živanov, O. Aleksić, S. Jenei, "Modeling and optimization of thick film solenoid-bar type inductors and transformers," *COMPEL*(*Computation and Mathematics in Electrical and Electronic Engineering*), vol. 19, no. 2, pp. 615-622, 2000.

[4] L. J. Golonka, "New application of LTCC technology," *28th Int. Spring Seminar on Electronics Technology,* pp. 148-152, 2005.

[5] L. J. Golonka, "Technology and application of Low Temperature Cofired Ceramic (LTCC) based sensors and mycrosystems," *Bulletin of the Polisch Academy of Sciences, Technical Sciences,* vol. 54, no. 2, pp. 221-331, 2006.

[6] Ansoft Inc. HFSS (High Frequency Structure Simulator). Pitssburg: Ansoft Corporation, 2002.

[7] http://www.dupont.com/mcm

[8] Đ. Vladisavljević, G. Radosavljević, A. Marić, G. Stojanović, Lj. Živanov, "Fizički model planarnog i 3D induktora projektovanih za LTCC tehnologiju," , *ETRAN, Subotica, Jun 2008.*

[9] V. Desnica, "Modelovanje i optimizacija planarnih debeloslojnih induktora solenoidnog tipa," Magistarski rad, Novi Sad, Novembar 1999.